

## $^8\text{Li}^+$ $\beta$ -NMR in the Cubic Insulator MgO

W A MacFarlane<sup>1</sup>, T J Parolin<sup>1</sup>, D L Cortie<sup>1,2,3</sup>, K H Chow<sup>4</sup>,  
M D Hossain<sup>2</sup>, R F Kieff<sup>2</sup>, C D P Levy<sup>5</sup>, R M L McFadden<sup>1</sup>,  
G D Morris<sup>5</sup>, M R Pearson<sup>5</sup>, H Saadaoui<sup>2,6</sup>, Z Salman<sup>5,6</sup>, Q Song<sup>2</sup>  
and D Wang<sup>2</sup>

<sup>1</sup> Chemistry Department, University of British Columbia, Vancouver, BC, V6T 1Z1, Canada

<sup>2</sup> Department of Physics and Astronomy, University of British Columbia, Vancouver, BC, V6T 1Z1, Canada

<sup>3</sup> Quantum Matter Institute, University of British Columbia, Vancouver, BC, V6T 1Z1, Canada

<sup>4</sup> Department of Physics, University of Alberta, Edmonton, AB, T6G 2E1, Canada

<sup>5</sup> TRIUMF, Vancouver, B.C. Canada, V6T 2A3

E-mail: [wam@chem.ubc.ca](mailto:wam@chem.ubc.ca)

**Abstract.** We present extensive high magnetic field  $\beta$ -NMR measurements of  $^8\text{Li}^+$  implanted in single crystals of MgO. The narrow resonance, consistent with a cubic  $^8\text{Li}^+$  site, likely the tetrahedral interstitial, is used routinely as a reference for shift measurements. We show the intrinsic linewidth is on the order of 200 Hz, allowing a frequency determination to an accuracy of a few Hz. We find no implantation energy dependence of the resonance within a few ppm, but there is evidence of slow spin dynamics in hole-burning measurements. The spin lattice relaxation is slow. The temperature dependence reveals interesting changes at low temperature whose origin remains uncertain.

### 1. Introduction

The high field  $^8\text{Li}^+$   $\beta$ -NMR resonance in rocksalt MgO is very narrow, with minimal nuclear dipolar broadening and no quadrupolar splitting, the latter implying a site with cubic symmetry for the implanted ion. The resonance in MgO is commonly used as a  $\beta$ -NMR frequency reference, from which the resonance shifts in other materials are measured. It will also serve as a useful reference for  $^{31}\text{Mg}$   $\beta$ -NMR[1] currently being developed at both ISAC and ISOLDE. Here the implanted ion will be isotopic with the stable Mg in the host. MgO is often used as a film growth substrate, and may have interesting magnetic properties when doped[2] or at surfaces[3]. It is also an important comparison with other rocksalt compounds such as EuO and LiF. Li doped MgO (MgO:Li) is also useful as a heterogeneous catalyst[4], and aside from chemical doping routes,  $\text{Li}^+$  ion implantation has also been studied recently as a means to modify MgO[5]. In this context, local information on the Li site and defect electronic structure for truly isolated  $\text{Li}^+$  would be a valuable addition to understanding MgO:Li. Here we report extensive characterization of the  $^8\text{Li}^+$   $\beta$ -NMR in MgO in high magnetic field.

<sup>6</sup> Present address: Paul Scherrer Institute, Laboratory for Muon Spin Spectroscopy, 5232 Villigen PSI, Switzerland



## 2. Experiment

$\beta$ -NMR experiments were carried out at the Isotope Separator and Accelerator (ISAC) facility at TRIUMF between 2002 and 2013. The  $^8\text{Li}^+$  has nuclear spin  $I = 2$ , radioactive lifetime  $\tau = 1.21$  s, gyromagnetic ratio  $\gamma = 6.3015$  MHz/T, and a small electric quadrupole moment  $Q = +31.4$  mb. A highly polarized beam of  $^8\text{Li}^+$  was implanted in the sample with a typical flux of  $10^6/\text{s}$  into a beam spot  $\sim 2$  mm in diameter. The implantation energy was varied by biasing the spectrometer to high positive voltage, thus electrostatically decelerating the incident  $^8\text{Li}^+$  beam from its transport energy (typically 20 or 30 keV). The nuclear polarization is monitored through the anisotropic  $\beta$ -decay of the highly polarized  $^8\text{Li}$  in two fast plastic scintillation detectors up- (B) and down- (F) stream of the sample. Resonances were measured with a continuous beam by introducing a transverse RF magnetic field,  $B_1$ , either as CW or modulated pulses, and scanning the frequency through the Larmor frequency at a rate slow compared to  $\tau$ . On resonance, the  $^8\text{Li}^+$  precess about  $B_1$  and the beta decay asymmetry is consequently reduced. To measure the spin lattice relaxation rate, the incoming  $^8\text{Li}^+$  beam was pulsed with a fast electrostatic kicker in the absence of any RF, and the relaxation of the beta decay asymmetry was monitored during and after the beam pulse. In each type of measurement both spin directions of the  $^8\text{Li}^+$  (parallel and antiparallel) relative to the large static field  $B_0$ , produced by a high homogeneity superconducting solenoid, were collected by alternating the helicity of the polarizing laser light. This has a number of advantages, including determination of the baseline of the helicity combined asymmetry. The field  $B_0$  ranged from 1.3 to 6.55 T.

We present data on a number of epitaxially polished MgO single crystals labelled F and R (supplier: Crystal GmBH, Berlin), M (supplier: MTI Corp., Richmond, CA), C1 and C2 (capped in situ with epitaxial Ag layers 19 and 29 nm thick).

## 3. Results and Discussion

The NMR of  $^8\text{Li}^+$  implanted in MgO consists of a single narrow resonance near the Larmor frequency in the applied field, with no evidence of quadrupolar splitting, implying a site of cubic symmetry. Power broadening (familiar from RF $\mu$ SR[6]) is clearly evident in the resonances with CW RF in Fig. 1. The Lorentzian linewidth (HWHM throughout), shown in Fig. 2, can be

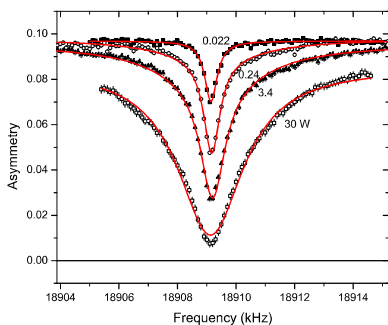


**Figure 1.** The CW resonance of  $^8\text{Li}^+$  implanted into MgO (3 T, 300 K, 30 keV) at different RF powers.

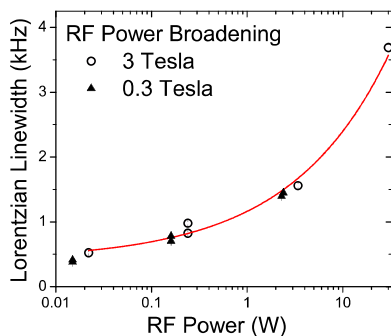


**Figure 2.** The Lorentzian linewidths of the data of Fig. 1 as a function of the RF power.

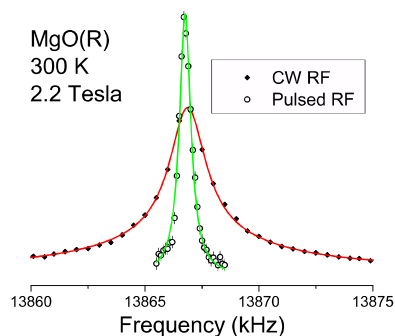


**Figure 3.** CW vs pulsed resonances at 19 keV into MgO sample R.

extrapolated to the zero power limit of  $w_0 = 407(160)$  Hz, independent of  $B_0$ <sup>7</sup>. This intrinsic linewidth is small on the scale of typical nuclear dipolar widths since MgO has small nuclear

<sup>7</sup> The resonance is better fit by the sum of two Lorentzian lines sharing the same frequency, but with different widths

moments in low abundance. However, use of a pulsed RF mode leads to a substantially narrower resonance (Fig. 3) of width 190(16) Hz, independent of  $B_0$  up to 6.55 Tesla. The difference is likely the result of spin dynamical effects in the CW resonance that are suppressed by the short RF pulses (see below).

We use the narrow resonance in MgO as a frequency reference for shifts of in other materials, so it is interesting to consider how close the resonance frequency is to the free Larmor frequency  $\nu_L$ . We expect the  ${}^8\text{Li}^+$  chemical shift to be small (on the order of a few ppm) as it is generally for Li NMR, e.g. see Ref. [7]. We should, however, consider demagnetization. Approximating the sample as a thin plate in a perpendicular field, the shift *correction* due to demagnetization is[8]

$$K_d = \frac{8\pi}{3}\chi, \quad (1)$$

where  $\chi$  is the dimensionless CGS volume susceptibility. MgO is weakly diamagnetic[9], with  $\chi = -1.38 \times 10^{-6}$ , yielding  $K_d = -11.5$  ppm, i.e. the resonance in MgO is shifted slightly up in frequency from  $\nu_L$ . This correction is important for determining small *absolute* shifts, e.g. the Knight shift in a metal where an accurate zero is required, especially if that shift is used in forming the Korringa ratio.

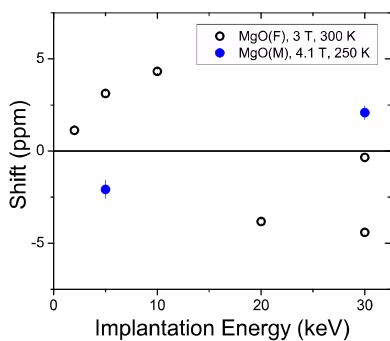


**Figure 4.** The shift of the resonance as a function of  ${}^8\text{Li}^+$  implantation energy, referred to zero on average.

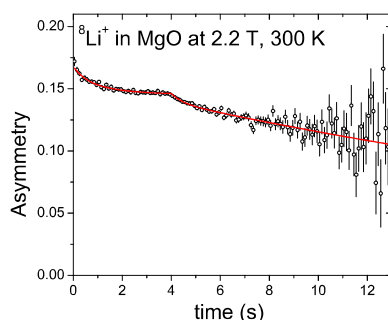


**Figure 5.** Spin lattice relaxation of  ${}^8\text{Li}^+$  in MgO(R) at 2.2 Tesla, 300 K, 20 keV.

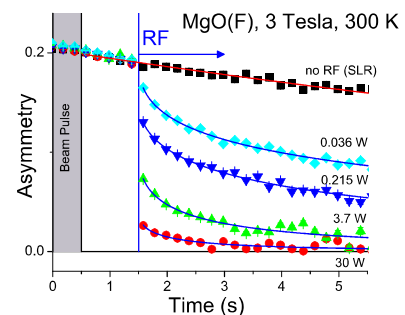


**Figure 6.** Hole burning measurements in MgO(F), see text.

A key strength of implanted ion  $\beta$ -NMR is the ability to vary the implantation energy  $E$  and hence implantation depth of the probe ions, thus obtaining *depth resolution*. A scan of  $E$  in MgO, shown in Fig. 4, reveals the resonance shift is depth independent (within 5 ppm), establishing an important comparison case for nontrivial *topological* insulators, such as some Bi compounds[10, 11], where depth dependence due to topological surface states is expected. Note that the statistical errors from the fits are much smaller than the scatter in the data, indicating that systematics are dominating the uncertainty in the resonance position. This is typically the case in these high rate experiments. Systematic drifts in the baseline asymmetry can result from fluctuations of the  ${}^8\text{Li}^+$  beam.

Spin lattice relaxation (SLR) of  ${}^8\text{Li}^+$  in MgO at high magnetic fields is slow. Fig. 5 shows data for a 4 s pulse of beam fit to a biexponential relaxation. We attribute the large slow relaxing signal to MgO, here with rate  $\lambda = 1/T_1 = 0.0312(29) \text{ s}^{-1}$ . The small fast component is likely a background signal.

While no RF is used in the SLR measurement, we can apply RF at a specific time during such a measurement. If the RF is on resonance, it causes a sudden downward step in the asymmetry,

of height proportional to the fraction of the line affected by the RF. A higher RF power thus leads to a larger step. However, if there are spin dynamics in the resonance, i.e.  $^8\text{Li}$  correspond to more than one unique frequency (within the resonance) during their lifetimes, then the RF has further effects. Spectral dynamics (diffusion) can be caused by  $^8\text{Li}^+$  motion and/or host nuclear spin fluctuations. With the RF applied continuously at a fixed frequency, one continues to destroy the polarization of any  $^8\text{Li}^+$  that stray into the “hole” that the RF “burns” into the resonance, leading to another mechanism of relaxation in the presence of the RF. Hole-burning measurements, where the RF is applied continuously 1 second after a 0.5 s pulse of beam are shown in Fig. 6. At the highest power (30 W), almost all the  $^8\text{Li}^+$  asymmetry is destroyed instantly. The step is reduced with reduced power, but there also appears a new time dependent relaxation that is much faster than the intrinsic SLR (also shown), caused by spectral diffusion. This effect has been used in conventional NMR, for example, to study slow diffusion[12]. A simple small frequency step random walk model predicts a relaxation proportional to  $\exp(-\sqrt{\Gamma t})$ . The relaxation after the RF is turned on is fit to a fraction relaxing at the intrinsic  $1/T_1$  plus such a term (blue curves). The hole-burning relaxation rate  $\Gamma$  is found to be  $1.2(7) \text{ s}^{-1}$ . This dynamic relaxation acts to increase the effective width of a resonance under CW RF, while pulsed RF, to the extent that the pulses are fast on the time scale of  $\Gamma$  is unaffected. This likely accounts for the substantially smaller pulsed RF linewidth mentioned above.

We now consider possible mechanisms for spectral diffusion.  $^{25}\text{Mg}$  is a low moment nucleus unfavourable for NMR, but some limited results are available[13, 14]. Its  $T_1$  is about 50 s at 300 K[14], much slower than  $\Gamma$ , but it is possible that the transverse relaxation time  $T_2$  is significantly faster and might account for the timescale  $\Gamma$ . Alternatively,  $^8\text{Li}^+$  may hop between equivalent lattice sites on the second timescale at 300 K. The distinction between these two mechanisms may be made from the temperature dependence, with the hop rate exhibiting an activated behaviour while  $T_2$  should be roughly  $T$  independent. As has been found in conventional NMR, hole-burning may provide a useful probe of very slow motion of the probe  $^8\text{Li}^+$ .

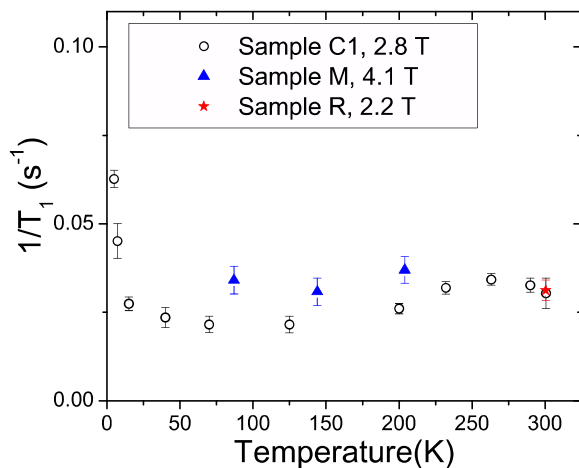


**Figure 7.** Spin lattice relaxation of  $^8\text{Li}^+$  at high fields as a function of temperature in several samples.

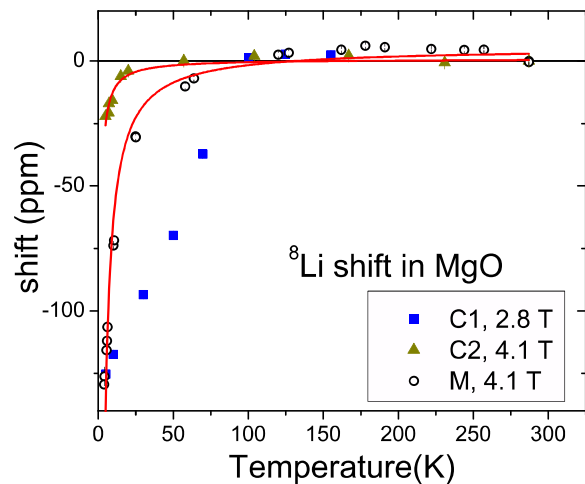


**Figure 8.** The temperature dependence of the shift of the  $^8\text{Li}^+$  resonance with respect to 300 K. The fits shown are to a (negative) Curie law plus a constant.

We have also measured the temperature dependence of both SLR and the shift (Figs. 7 and 8) that reveal an increase in  $1/T_1$  at low temperature and a negative shift of the resonance below 100 K that increases as temperature is lowered. The origin of these changes at low temperature is not clear, but here we consider some possibilities.

Magnetic impurities in the MgO would cause a negative demagnetization shift via Eq. (1) with a uniform paramagnetic  $\chi$ ; however, the concentration of such defects required to account for the observed shift seems unreasonably high (at the % level). Moreover, such a concentration should cause significant broadening of the resonance, while only a modest broadening is found.

Studies of Li doped MgO find that substitutional  $\text{Li}'_{\text{Mg}}$  localizes a hole, i.e. the  $[\text{Li}]^0$  centre[15]. As  $\text{Li}^+$  is negatively charged relative to the  $\text{Mg}^{++}$  that it replaces, there is a Coulomb attraction for positive mobile charges, and at low temperatures an oxygen  $2p$  hole is localized on the near neighbours of the Li defect. The holes are provided by high energy irradiation or by quenching[16]. EPR[15, 17, 18] and ENDOR[19] find a negative hyperfine field on the Li nucleus[20, 21], and a significant anisotropy due to relaxation of the lattice with respect to the  $\text{Li}^+-\text{O}^-$  axis, breaking local cubic symmetry[15, 19]. The isotropic part of the hyperfine interaction with the hole spin is found to be  $-4.539$  MHz[19]. The disappearance of anisotropy with increasing temperature was interpreted as a result of slow hopping of the hole among the neighbouring oxygen ions[18, 19]. This picture was supported by several theoretical calculations[21, 22, 23] and is quite different from a symmetric localized state predicted more recently for Ca vacancies in CaO[24].

There are a number of problems attributing the negative  $^8\text{Li}$  shift at low temperature to such a localized hole. In particular, we see no evidence of a noncubic environment at the  $^8\text{Li}^+$ , and, rather than a large hyperfine field, we have only a small shift on the scale of 100 ppm compared to the hyperfine field from ENDOR which corresponds to more than  $10^5$  ppm at 4.1 T. This is somewhat reminiscent of Mu in heavily  $n$  type Si[25], where the shift is the remnant of the Muonium hyperfine field reduced by averaging due to rapid exchange of the Mu electron with the surrounding conduction electrons at densities on the order of  $10^{18}/\text{cm}^3$ . In MgO, there is no such bath of mobile electrons, unless there is a significant transient population of carriers related to the implantation itself. The density of implantation-related carriers would have to be quite high in the vicinity of the stopped  $^8\text{Li}^+$  to make this mechanism feasible. The sample dependence in Fig. 8 is also not easy to explain in this picture.

Finally, it is not even clear that the implanted  $^8\text{Li}^+$  is at the substitutional site. In many materials, we find substitutional  $^8\text{Li}^+$  only at high temperature. At low temperatures,  $^8\text{Li}^+$  is generally in a metastable interstitial site. Such a site is available here, the tetrahedral interstitial ( $T$ ) site. Based on effective ionic radii in oxides, the  $T$  site is too small to accommodate  $\text{Li}^+$ , and significant outward relaxation of the 4 neighbouring  $\text{O}^{2-}$  would be necessary. Our initial density functional calculations suggest that this is a higher energy site for  $^8\text{Li}^+$  than the Mg site, but in the absence of a Mg vacancy, this may well be the only available cubic site. Unlike  $\text{Li}'_{\text{Mg}}$ ,  $\text{Li}_T$ , is a positive defect that would tend to localize an electron (rather than a hole), and this is not likely on the neighbouring  $\text{O}^{2-}$ .

Further experiments and calculations are necessary to characterize the electronic structure of the implanted  $^8\text{Li}^+$  in MgO.

#### 4. Summary

We have presented extensive results on the  $\beta$ -NMR of  $^8\text{Li}^+$  implanted in cubic MgO, where it occupies a cubic site, likely the tetrahedral interstitial site. We routinely use the narrow resonance as a reference for resonance shifts, and we show here that the intrinsic linewidth is on the order of 200 Hz, which allows a reference frequency to be measured to an accuracy of a few Hz. We find no implantation energy dependence of the resonance within a few ppm, but we find evidence of slow spin dynamics at 300 K from hole-burning measurements. The temperature dependence reveals interesting changes at low temperature whose origin remains uncertain.

## Acknowledgments

We thank S. Hak and T. Hibma of the University of Groningen for samples C1 and C2; the TRIUMF CMMS and ISAC facility for technical support; and S.X.Y. Wang for the spectral diffusion modeling.

## References

- [1] Kowalska M, Yordanov D T, Blaum K, Himpe P, Lievens P, Mallion S, Neugart R, Neyens G and Vermeulen N 2008 *Phys. Rev. C* **77** 034307
- [2] Elfimov I S, Rusydi A, Csiszar S I, Hu Z, Hsieh H H, Lin H J, Chen C T, Liang R and Sawatzky G A 2007 *Phys. Rev. Lett.* **98** 137202
- [3] Gallego S, Beltrán J I, Cerdá J and Muñoz M C 2005 *J. Phys. Cond. Matt.* **17** L451
- [4] Arndt S, Laugel G, Levchenko S, Horn R, Baerns M, Scheffler M, Schlögl R and Schomäcker R 2011 *Catalysis Reviews* **53** 424–514
- [5] Tardío M M, Ramírez R, González R and Chen Y 2002 *Phys. Rev. B* **66** 134202
- [6] Kreitzman S 1991 *Hyp. Int.* **65** 1055–1069
- [7] Böhmer R, Jeffrey K and Vogel M 2007 *Prog. NMR Spectrosc.* **50** 87–174
- [8] Xu M, Hossain M, Saadaoui H, Parolin T, Chow K, Keeler T, Kiefl R, Morris G, Salman Z, Song Q, Wang D and MacFarlane W 2008 *J. Magn. Reson.* **191** 47–55
- [9] Candea R M, Hudgens S J and Kastner M 1978 *Phys. Rev. B* **18** 2733–2738
- [10] MacFarlane W *et al.* In preparation
- [11] Koumoulis D *et al.* In preparation
- [12] Kuhns P L and Conradi M S 1982 *J. Chem. Phys.* **77** 1771–1778
- [13] Dupree R and Smith M E 1988 *J. Chem. Soc., Chem. Commun.* 1483–1485
- [14] Fiske P, Stebbins J and Farnan I 1994 *Physics and Chemistry of Minerals* **20** 587–593
- [15] Schirmer O 1971 *J. Phys. Chem. Sol.* **32** 499–509
- [16] Abraham M M, Chen Y, Boatner L A and Reynolds R W 1976 *Phys. Rev. Lett.* **37** 849–852
- [17] Halliburton L E, Kappers L A, Cowan D L, Dravnieks F and Wertz J E 1973 *Phys. Rev. Lett.* **30** 607–610
- [18] Sanjuan M L and Orera V M 1986 *J. Phys. C* **19** 67
- [19] Abraham M M, Unruh W P and Chen Y 1974 *Phys. Rev. B* **10** 3540–3545
- [20] Bass R 1984 *Phys. Rev. B* **30** 5334–5335
- [21] Lichanot A, Larriue C, Zicovich-Wilson C, Roetti C, Orlando R and Dovesi R 1998 *J. Phys. Chem. Sol.* **59** 1119–1124
- [22] Zuo J, Pandey R and Kunz A B 1991 *Phys. Rev. B* **44** 7187–7191
- [23] Shluger A L, Kotomin E A and Kantorovich L N 1986 *J. Phys. C* **19** 4183
- [24] Elfimov I S, Yunoki S and Sawatzky G A 2002 *Phys. Rev. Lett.* **89** 216403
- [25] Chow K H, Kiefl R F, Hitti B, Estle T L and Lichti R L 2000 *Phys. Rev. Lett.* **84** 2251–2254